Desalination and Water Treatment
www.deswater.com

43 (2012) 43–51
April

1944-3994/1944-3986 © 2012 Desalination Publications. All rights reserved
doi: 10.1080/19443994.2012.672197

Taylor & Francis
Taylor & Francis Group

New chitosan/poly (acrylic acid) composite membrane for application in pervaporation dehydration of caprolactam solution

Qin Li[a,b], Wenhai Lin[a], Tianrong Zhu[a], Yunbai Luo[a], Ping Yu[a,*]

[a]*College of Chemistry and Molecule Science, Wuhan University, Wuhan 430072, P.R. China*
Tel. +86 27 68752469; Fax: +86 27 68776726; email: yuping@whu.edu.cn
[b]*Anhui Electric power Design Institute, Hefei, Anhui 230601, P.R. China*

Received 26 February 2011; Accepted 8 February 2012

ABSTRACT

To improve caprolactam pervaporation (PV) separation dehydration process, composite membrane was investigated using chitosan (CS) and poly (acrylic acid) (PAA) blending membrane as active layer and a polyacrylonitrile (PAN) ultrafiltration membrane as substrate. The composite membranes were characterized by FTIR, SEM, and XRD measurements to assess the intermolecular interactions membranes of morphology, and observe the crystallinity, respectively. The effect of the ratio of PAA and CS in the composite membranes on the PV performance was investigated. The flux was decreased and the separation factor was increased by the PAA content increase in the range of 10–30 wt.%. Besides, operating temperature and feed composition on PV performances were investigated. Data showed that PAA/CS composite membranes displayed good swelling and PV performance, and the composite membranes had superior separation performances for dehydration of ε-caprolactam solution, that the highest separation factor could reach 7,804 at 313 K, for 70 wt.% caprolactam. The evaluated results revealed that the separation performances of CS/PAA composite membranes were strongly related to their reaction degree and intrinsic structure as well as the operating parameters.

Keywords: Chitosan; Poly (acrylic acid); ε-Caprolactam; Pervaporation

1. Introduction

Pervaporation (PV) technique is an eco-friendly and economical separation method compared to conventional separation processes for close-boiling, azeotropic, isomeric, or heat-sensitive liquid mixtures in the chemical industry [1–6]. Traditional separation techniques for the ε-caprolactam (CPL) purification, such as crystallization, thin-film distillation, and melt crystallization by suspension, have many disadvantages, especially low heat transfer coefficient, a large amount of middle pressure steam consumption from steam containing considerable CPL. Therefore, our group introduced PV technique into the CPL purification using polyvinyl alcohol (PVA) membrane [7]. But PVA is a linear chain structure polymer, has high crystallization and high orientation, limited further improvement in the separation factor [8].

Chitosan (CS) is the most abundant biopolymer in the nature [9–11]. CS has both reactive amino and hydroxyl groups that have a good hydrophilic nature. It also has good film-forming properties, chemical resistance and high selectivity for water solution. CS was widely used in PV separation of aqueous–organic mixtures [12,13]. In previous works, we found that CS–PVA blending composite membranes used in CPL–water system on PV had better separation factor than PVA membranes [14,15]. Poly (acrylic acid)

*Corresponding author.

(PAA) is an anionic polymer applied to membrane separation processes beginning in the 1960s [16–20]. Nam and Lee blends of PAA and CS for composite membranes in the PV the dehydration of alcohols [21]. Electrostatic interaction has to be formed by mixing of positively and negatively charged polyions in aqueous medium. This property of PAA may improve the CS membrane separation factor.

The present work explores the performance of these PAA–CS composite membranes of different blending ratios for the separation of CPL–water mixtures. The morphological structure, thermal stability, and mechanical properties of the modified films characterization were carried out using infrared (IR), wide-angle X-ray diffraction (XRD), derivative thermogravimetric curve (DTG), scanning electron microscope (SEM), and swelling test. The relationship between the structure and their physicochemical properties has been discussed. The effect of PV operating parameters such as temperature and feed concentration has been evaluated. In addition, the work also sought to find out whether PAA–CS composite film in the paper would have the desired separative duty for CPL solution.

2. Experimental

2.1. Materials

CPL (industrial grade) was supplied by Baling Petrochemical Co. Ltd (SINOPEC, China); PAA of molecular weight 1,000 and CS having an average molecular weight 500,000 were purchased from Guoyao Chemicals Co., Ltd (Si Chuan, China). The degree of deacetylation of CS was found to be 91%. Other chemicals were of reagent grade and used without further purification.

Porous ultrafiltration membrane of polyacrylonitrile (PAN) (Cut-off MW 5×10^4) was supplied by the Development Center of Water Treatment Technology (China). Deionized water was used in preparing the aqueous feed solutions for the PV experiments.

2.2. Preparation of crosslinked composite membranes

CS was dissolved in deionized water to prepare a concentration of 1 wt.% solution. To this solution, series amount (10, 20, and 30 wt.% of the solute) of PAA was added and the reaction lasted for 24 h. The resulting homogeneous solution was used for the sequent process after degassing.

The coated membranes, hydrolyzed PAN microporous membranes, were prepared by immersing PAN ultrafiltration membrane in 5 wt.% NaOH aqueous solution at 50°C for 1 h, washed thoroughly with deionized water until neutral and then immersed in 1 N HCl aqueous solution for 20 min, and washed with water until neutral [14]. Then, the prepared solution was cast on the porous PAN substrate membranes held on a glass plate. The composite membranes in the gelatination state were allowed to evaporate slowly in a dust-free atmosphere till dried at ambient temperature. Finally, the composite membranes were treated in an air-circulating oven to effect thermal crosslinking structure. This chemical crosslinking reaction is displayed in Fig. 1. The membranes in different PAA mass ratio (10, 20, and 30 wt.% of the total solute) were designated as M1, M2, and M3, respectively, as Table 1.

2.3. Swelling experiments

Equilibrium swelling experiments on all membranes were performed in feed mixtures of CPL/water with compositions ranging from 30 to 70 wt.% water at 40°C. The masses of dry membranes were first determined and these were equilibrated by soaking in different compositions of feed mixture in a sealed vessel for 48 h. All the experiments were performed at least three times and the results were averaged. The percent degree of swelling (S) was calculated by the following equation:

$$S(\%) = (W_s - W_d)/W_d \times \% \quad (1)$$

where W_d and W_s are the weights of dry membrane and swollen membrane, respectively.

2.4. Characterization

2.4.1. Fourier transform infrared (FT-IR) spectroscopy

The crosslinking reaction of CS/PAA with GA was confirmed by the FT-IR spectroscopy. The FT-IR spectra of various composite membranes were scanned using Nicolet AVATAR 360 FT-IR spectrometer.

2.4.2. Scanning electron microscopy

The morphology of the various composite membranes was examined by SEM. All specimens were coated with a conductive layer of sputtered gold. The morphologies of the CS/PAA composite membranes were observed with SEM (FEI Quanta 200, Holland).

2.4.3. XRD analysis

XRD measurements were analyzed using a Shimadzu XRD-6000 (Japan) diffractometer equipped

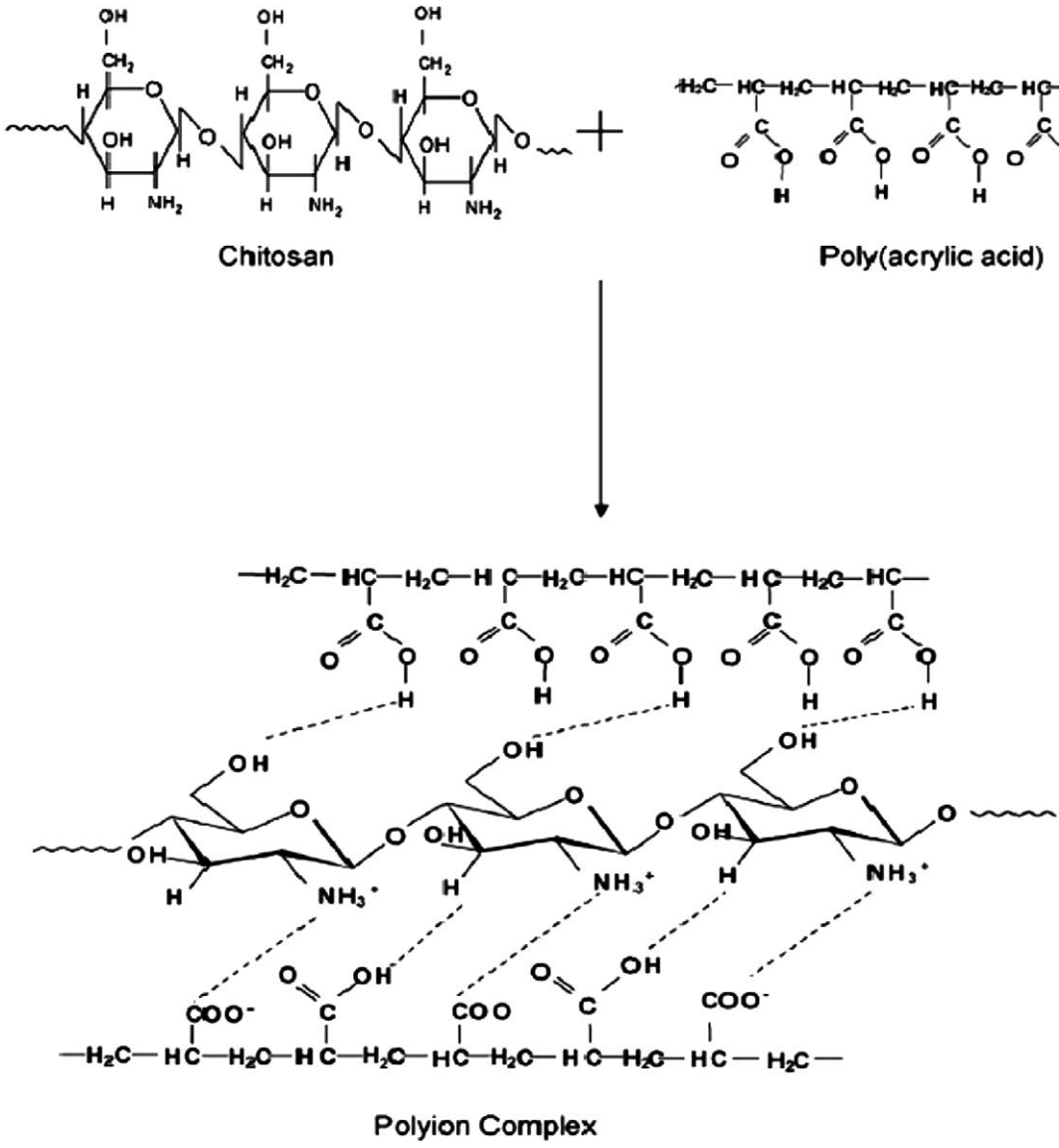

Fig. 1. The chemical crosslinking reaction of CS and PAA.

with graphite monochromatized Cu Kα radiation ($\lambda = 1.54060$ Å) at 40 kV and 30 mA with a scan rate of 4°/min. The angle of diffraction was varied from 5° to 45° to identify any changes in the crystal structure.

2.4.4. Thermal gravimetric analyses

Thermal gravimetric analysis was conducted with SETSYS 16 instrument (France) under a nitrogen atmosphere with a flow capacity of 50 mL/min. The scan was carried out at a heating rate of 10°C/min from 20 to 600°C. The sample weight was about 5–10 mg and analyzed using an a-Al_2O_3 crucible.

2.4.5. PV experiments

The tested membrane was allowed to equilibrate for about 1–2 h at the corresponding temperature before

Table 1
Typical sample preparation and designation of CS–PAA composites membrane

Membranes	Concentration (wt.%)	
	CS	PAA
M1	90	10
M2	80	20
M3	70	30

performing the PV experiment with fixed compositions of the feed mixture. After establishment of a steady state, the permeate vapor was collected in a trap immersed in the liquid nitrogen jar on the downstream side at a fixed time of intervals. The feed mixture was varied from 30 to 70 wt.% CPL and PV experiments were conducted in the range of 40–60°C [14].

From the PV data, separation performance of membranes was assessed in terms of flux (J) and separation factor (α). These were calculated, respectively, using the following equations:

$$\alpha = y_w x_{CPL}/x_w y_{CPL} \quad (2)$$

$$J = W/At \quad (3)$$

Where in Eq. (2) x_w, y_w are the mole fractions of water in the feed and permeate, and x_{CPL}, y_{CPL} are the mole fractions of CPL in the feed and permeate; in Eq. (3), W (g), A (m^2) and t (h) are the weight of permeates, effective membrane area, and time, respectively.

3. Results and discussion

3.1. Membrane characterization

3.1.1. FT-IR analysis

FT-IR spectra presented in Fig. 2 were the composite membranes prepared by blending CS and PAAc in various ratios. From this spectrum of pure CS (Fig. 2(a)), it can be seen that the absorption band of the stretching of –OH groups was at 3,388 cm^{-1} and the band at 1,650 predominantly arose from $–NH_2$ groups' asymmetric stretching. [22]. The adsorption peak at 1,064 cm^{-1} provided the evidence of characteristic absorption band of C_6–OH.

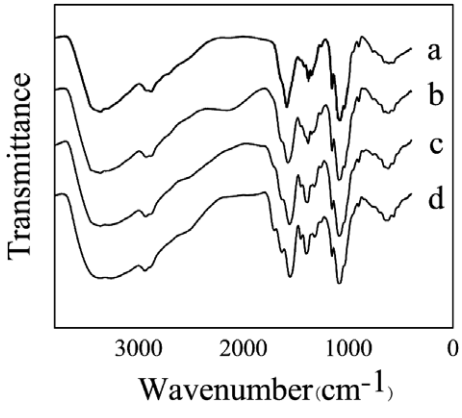

Fig. 2. FTIR spectra of pure CS (a) and composite membranes M1(b), M2(c), M3(d) with different PAA contents.

The peak at 1,727 cm^{-1} was dominated by the stretching of the C=O in the carbonyl of acetyl groups. From Fig. 2(b) to Fig. 2(d) a new peak at 1,550 cm^{-1} in the spectra of the composite membranes can be evidenced. This may be assigned to the symmetric NH_{3+} deformation resulting due to $–NH_2$ in CS reacting with –COOH groups in PAA. Broad peaks appearing at 1,800 cm^{-1} in the composite membranes also confirm the presence of COO^- as in PAA. The negatively charged carboxylate ion (COO^-) and positively charged NH_{3+} coexist in CS–PAA composite membranes [22]. Thus, the results of FT-IR analysis clearly prove the formation of the polyion composite membranes of the acid–base reaction. Compared with pure CS, it can be seen that the absorption band of the stretching of –OH groups in crosslinked membranes was narrower and the absorption frequency shifts to a lower wavenumber. It is suggested that the interaction between crosslinking agent and CS reduced the number of –OH groups, which can be also seen in the change of the peak at 1,635 cm^{-1}, indicating that crosslinking reaction reduced the number of hydrogen bonds [14]. FTIR results confirmed the crosslinking in the polymers.

3.1.2. SEM analysis

Fig. 3 shows the SEM micrographs of cross-section morphology for CS–PAA film. The multilayer structure of membrane was observed very clearly: an active layer and a supported porous layer, which was similar to the membrane studied by our former work [8]. It can be seen that the surface of active layer was smooth and compact without any cracks. The aperture of porous layer was also arranged very regularly, which was of benefit for the osmosis of the membranes and improvement of the flux [8]. The smooth surface of the film exhibited that a uniform CS–PAA thin dense layer with a thickness of about 10 μm is properly cast on the top of the PAN substrate in Fig. 3(a) and (b).

3.1.3. XRD analysis

The XRD patterns of the CS/PAA composite membranes are given in Fig. 4. As can be seen, XRD patterns of all the membranes indicate semicrystalline behavior. CS (Fig. 4(a)) exhibits a typical peak at $2\theta = 12°$ and 20° [23]. These two peaks are related to two types of crystals. The peak at 12° has notability effect on the properties of separation [24]. From these patterns, it is clear that the crystallinity has decreased with increasing PAA contents in the composition

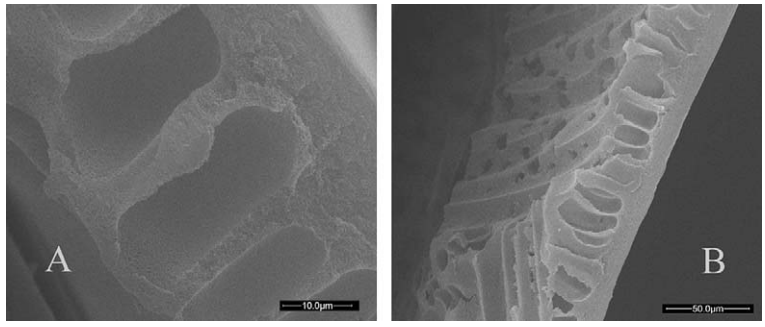

Fig. 3. The cross-section morphology of the CS–PAA composite membrane M1.

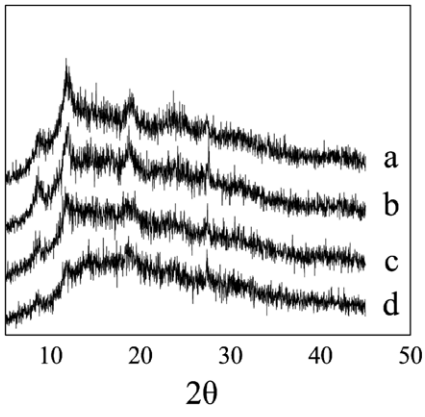

Fig. 4. XRD pattern of the CS–PAA composite membrane: (a) pure CS; (b) M1; (c) M2; (d) M3.

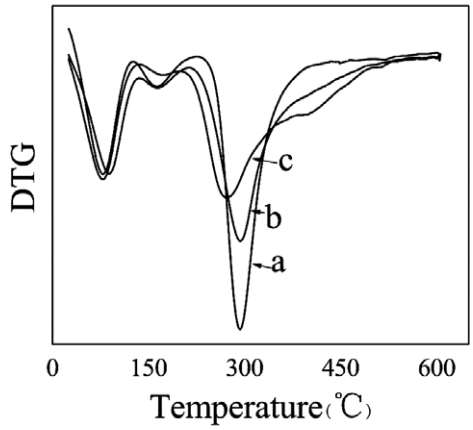

Fig. 5. DTG thermograms of the CS–PAA composite membranes: (a) M1; (b) M2; (c) M3.

membranes. This result implies that the change in the ratio of PAA and CS content changed the crystallinity of the membrane after reaction, whereas the CS/PAA composite membrane appeared to have greater amorphous morphology [22]. This may be due to the acid–base reaction resulting in blending the two polymers, which causes the destruction of hydrogen bonding between amino groups and hydroxyl groups in CS. Then the structure of the polymer was significant prior to water penetration through the membrane on PV. It was because the decrease of crystallinity reduced the diffusion resistance and increased free volume, helping to improve the penetration flux of each component [25]. In general, this result of XRD was in agreement with the result of FT-IR.

3.1.4. Thermal analysis

Thermal stability analysis of polymer material is helpful in the selection of materials with the best properties for specific used. Fig. 5 shows the thermal stability of CS/PAA composite membranes. M1 showed two main stage degradation peaks within the range of 100 and 300°C. Compared with M1, the degradation peaks of M2 and M3 in the range of 100 and 300°C reduce and the degradation thermal decomposition process moved to a high temperature zone, and along with the ratio increasing of PAA in the films. This is because the reaction between the CS with amino group and the PAA with carboxyl groups formed the acylamide bond that had better thermal stability. Compared with the M1 composite membranes used in the same system, increase of PAA in CS enhances the thermal stability of PV membranes [26].

3.2. PV characteristics

3.2.1. Swelling experiments

Fig. 6 shows the degree of swelling obtained by soaking the CS–PAA composite membranes in the different CPL concentration solution at 40°C. Sorption mechanism is an important factor for membrane swelling in PV process, as it controls the transport of permeating molecules under the chemical potential

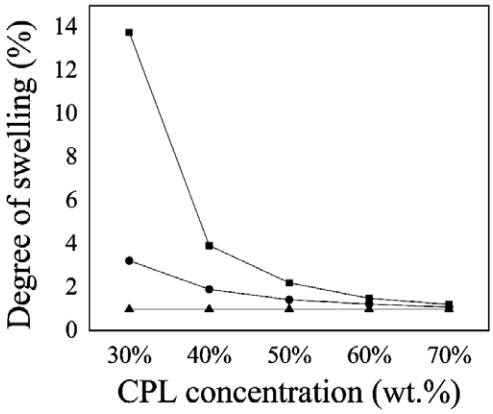

Fig. 6. Degree of swelling of the CS–PAA composite membranes at 40°C: ■M1; ●M2; ▲M3.

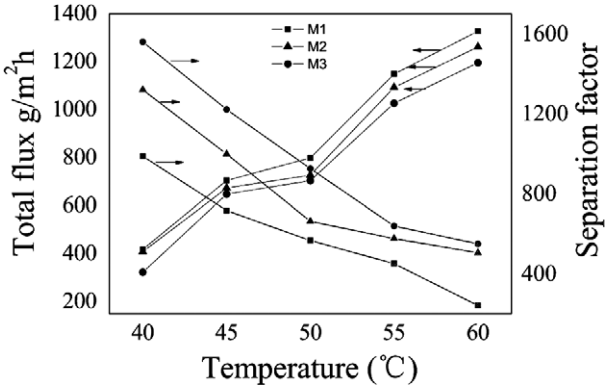

Fig. 7. Effect of the operating temperature on the PV performances in terms of total flux and separation factor at 30 wt.% CPL aqueous solution.

gradient. This section is to determine the influences of the degree of swelling in PV performance. Therefore, to study the effects of PAA ratio on membrane swelling, the degree of swelling was plotted with respect to different mass percent of CPL from 30 to 70% in the feed, we chose the data at 40°C as shown in Fig. 6.

It is noticed that the degree of swelling of the membranes M1and M2 decreased when the CPL content in the solution increased. This is due to the fact those membranes were hydrophilic and showed an increase of strong interaction between water molecules and the membrane containing –OH groups and NH_2 groups [22]. But the degree of swelling of the membrane M3 was found to be negligible in the different CPL concentration solutions. And at the same concentration solution, the degree of swelling reduced for the composite membranes with more PAA, due to the strengthened reaction with CS and PAA. More reaction between NH_2 groups and COOH groups formed more amide bonds, so that the activity of molecular chains reduced step by step, increasing the mechanical strength of the membranes but reducing the hydrophilic [8]. This means that when solvent molecules were absorbed with difficulty, it would reduce the degree of swelling of membranes sharply.

3.2.2. Effect of the operating temperature and content of PAA

The PV total flux and separation factor are influenced by the change in temperature sensitivity [27]. So we have typically chosen the condition of 30 wt.% of CPL in feed to study the temperature effects, and the resulting values are presented in Fig. 7.

The operating temperature range was chosen from 40 to 60°C [28]. As was reflected from the Fig. 7, it could be due to the fact that the total fluxes always increase with the increase of feed temperature, and this "trade-off" phenomenon may be traditionally explained by the increase in frequency and amplitude of polymer chain thermally induced expansion of the free volume in membranes [29]. The internal structures of the polymer highly influenced the free volume in the matrix and eventually affected the separation factor of the membranes [22]. Increase of smaller molecules penetrant diffusivities was the other source of this behavior. While the total fluxes showed an upward tendency following the temperature rising, the separation factor decreased synchronously (Fig. 7). It is because induced expansion of the free volume in membranes, permeants molecular passed easily [30]. In addition, with increasing feed temperature, the vapor pressure in the feed compartment increased, but the vapor pressure at the permeate side was not affected. These resulted in an increase of driving force with increasing temperature. Therefore, the permeation of diffusing molecules and the associated molecules through the membrane became easier, leading to an increase of total permeation flux, while suppressing the separation factor. Compared with PVA membranes [8], it could be found that CS–PAA composite membranes have a lower flux and higher separation factor under the same condition, with more PAA reacting with CS, due to the fewer active groups of unit mass and denser network structure, total flux lower more and separation factor more excellently. These results were simulation agree well with the test of FTIR and XRD. So the membranes of M1 have the best flux and M3 have the best separation factor. These results were

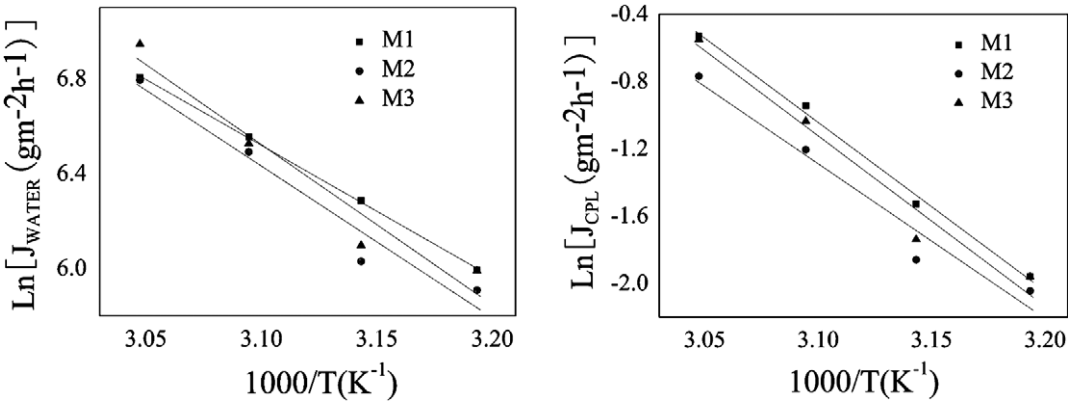

Fig. 8. Temperature dependence of (a) water and CPL flux, for 40 wt.% CPL concentration.

simulation agree well with the test of the degree of swelling.

3.2.3. Activation energy analysis

Temperature-dependent flux data have been fitted to the Arrhenius relationship to estimate the activation parameters. The Arrhenius relationship is expressed in Eq. (4).

$$J = J_0 \exp(-E_p/RT) \quad (4)$$

where J, g/(m^2 h), is the permeation flux; E_p, kJ/mol, is the activation energy for permeation; J_0, g/(m^2 h), is the permeation rate constant; T is the absolute temperature; and R is the molar gas constant. The activation energy (ΔE_a) of water and CPL permeates through the M1, M2, and M3 membranes with 40 and 50% CPL concentrations are calculated on the basis of the Arrhenius formula as shown in Fig. 8, and their results were summarized in Table 2. It could be found that activation energies of total flux and water permeations were nearly in each same membrane at the same feed concentration. It suggested water flux had a control of total flux. In addition, the activation energy for CPL permeation was higher than that for water permeation. It implied that water consumes less amount of energy for permeation and had higher permeability than CPL. It suggested that higher separation factor needs lower energy. The two activation energies of M1 were obviously lower for other membranes in this study. That fact proved M1 was the most easily permeation membrane at this concentration range.

Table 2
Activation energy data of M1, M2, and M3 in PV at 40 wt. % and 50 wt.% CPL aqueous solution

Feed concentration		Membrane type		
		ΔE_a activation energy (kJ/mol)		
		E_t	E_w	E_{CPL}
40 wt.%	M1	45.87	45.83	99.55
	M2	52.65	52.63	97.31
	M3	52.41	52.38	100.703
50 wt.%	M1	46.22	46.20	83.30
	M2	53.21	53.20	76.41
	M3	56.16	56.14	84.22

3.2.4. Effect of feed composition

Feed composition effect of flux and separation factor results are displayed in Fig. 9. Fig. 10 shows the effect of feed concentration on the total permeation

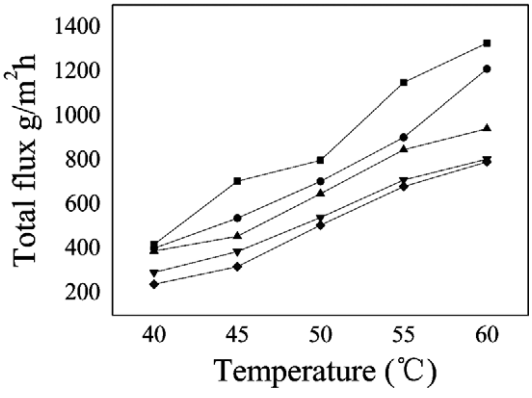

Fig. 9. Total flux and temperature vs. concentration of CPL (■70 wt.%; ●60 wt.%; ▲50 wt.%; ▼40 wt.%; ◆30 wt.%) in the feed for M1, M2, and M3 membranes.

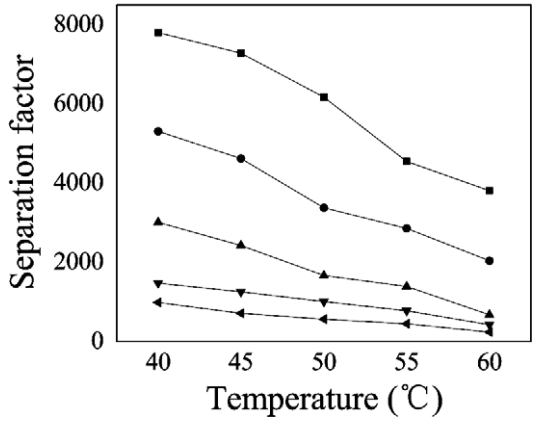

Fig. 10. Total flux and temperature vs. concentration of CPL (■70 wt.%; ●60 wt.%; ▲50 wt.%; ▼40 wt.%; 30 wt. %) in the feed for M1 membranes.

flux and separation factor vs. concentrations of 30–70 wt.% CPL in feed at different temperatures with M1 membranes. These figures indicate that flux and separation factors are also strongly dependent on the feed composition. It can be seen that the flux of M1 increased from 792 to 1,327 g/(m^2 h) for feeds containing 30–70 wt.%. The superiority of flux in lower CPL feed concentration and separation factor in higher CPL feed concentration were quite obvious. It is observed that the total permeation flux increased for the increase of mass percent of water in the feed. This behavior is same with the previous reports in the dehydration of aqueous organic mixture through blending polymer membranes [31,32]. Such flux results are due to the membranes swelling greatly at a higher concentration of water in the feed, increasing flux. As a result, the separation factor decreased gradually at a higher concentration of water in the feed. The trend is the same as in our former work [8,14] and CS/PAA membranes have the obvious advantage in separation factor. This phenomenon can be explained by the water concentration in the feed increasing, the amorphous regions of the CS/PAA crosslink structure becoming more flexible and more swollen, both water and CPL molecules bringing about diffusion more easily across the membranes. So the flux increased and the separation factor decreased. This is known as the trade-off rule that was generally observed in other PV processes [33,34].

4. Conclusions

CS/PAA composite membranes were prepared and the PV dehydration experiment was conducted. The introduction of PAA changed the structure of the CS polymer chain, and then affected the PV performance of the composite membranes. FTIR spectra and XRD curves showed the changes of structure, and SEM displayed the morphology of the composite membranes. The reaction of PAA and CS decreased the membranes' hydrophilicity and increased the thermal stability of the membranes. With increasing the PAA content, the permeation separation factor increased with a drop of flux. With increasing of both temperature and feed water concentration, the total flux increased and the separation factor decreased. Swelling results followed the same trends. Meanwhile, the application of CS/PAA composite membranes in CPL/water system on PV was successful. The data showed that the improved separation factor for CPL/water. The experimental results also indicated that the CS/PAA composite membrane had superior dehydration performances for caprolactam solution.

References

[1] D.J. Upadhyay, N.V. Bhat, Separation of azeotropic mixture using modified PVA membrane, J. Membr. Sci. 255 (2005) 181–186.
[2] F.R. Chen, H.F. Chen, Pervaporation separation of ethylene glycol–water mixtures using crosslinked PVA–PES composite membranes: Part I. Effects of membrane preparation conditions on pervaporation performances, J. Membr. Sci. 109 (1996) 247–256.
[3] A.S. Ariyaskul, R.Y.M. Huang, P.L. Douglas, R. Pal, X. Feng, P. Chen, L. Liu, Blended chitosan and polyvinyl alcohol membranes for the pervaporation dehydration of isopropanol, J. Membr. Sci. 280 (2006) 815–823.
[4] L.Y. Wang, J.D. Li, Y.Z. Lin, C.X. Chen, Separation of dimethyl carbonate/methanol mixtures by pervaporation with poly(acrylic acid)/poly(vinyl alcohol) blend membranes, J. Membr. Sci. 305 (2007) 238–246.
[5] D.A. Devi, B. Smitha, S. Sridhar, T.M. Aminabhavi, Pervaporation separation of dimethylformamide/water mixtures through poly(vinyl alcohol)/poly(acrylic acid) blend membranes, Sep. Purif. Technol. 51 (2006) 104–111.
[6] D.J. Lin, C.L. Chang, H.Y. Shaw, Y.S. Jeng, L.P. Cheng, Formation of multilayer poly(acrylic acid)/poly(vinylidene fluoride) composite membranes for pervaporation, J. Appl. Polym. Sci. 93 (2004) 2266–2274.
[7] L. Zhang, P. Yu, Y.B. Luo, Comparative behavior of PVA/PAN and PVA/PES composite pervaporation membranes in the pervaporative dehydration of caprolactam, J. Appl. Polym. Sci. 103 (2007) 4005–4011.
[8] L. Zhang, P. Yu, Y.B. Luo, Dehydration of caprolactam–water mixtures through cross-linked PVA composite pervaporation membranes, J. Membr. Sci. 306 (2007) 93–102.
[9] T. Uragami, K. Takigawa, Permeation and separation characteristics of ethanol–water mixtures through chitosan derivative membranes by pervaporation and evapomeation, Polymer 31 (1990) 668–672.
[10] T. Uragami, T. Matsuda, H. Okuno, T. Miyata, Structure of chemically modified chitosan membranes and their characteristics of permeation and separation of aqueous ethanol solutions, J. Membr. Sci. 88 (1994) 243–251.
[11] M. Nawawi, M. Ghazali, R.Y.M. Huang, Pervaporation dehydration of isopropanol with chitosan membranes, J. Membr. Sci. 124 (1997) 53–62.
[12] M.B. Patil, T.M. Aminabhavi, Pervaporation separation of toluene/alcohol mixtures using silicalite zeolite embedded chitosan mixed matrix membranes, Sep. Purif. Technol. 62 (2008) 128–136.

[13] R.S. Veerapur, K.B. Gudasi, T.M. Aminabhavi, Pervaporation dehydration of isopropanol using blend membranes of chitosan and hydroxypropyl cellulose, J. Membr. Sci. 304 (2007) 102–111.
[14] Q. Li, P. Yu, T.R. Zhu, L. Zhang, Q. Li, Y.B. Luo, Pervaporation performance of crosslinked PVA and chitosan membranes for dehydration of caprolactam solution, Desalination 16 (2010) 304–312.
[15] N.D. Hilmioglu, S. Tulbentci, Pervaporation of MTBE/methanol mixtures through PVA membranes, Desalination 160 (2004) 263–270.
[16] A.S. Micheals, Polyelectrolyte complexes, Ind. Eng. Chem. 57 (1965) 32–40.
[17] X.Y. Qu, H. Dong, Z.J. Zhou, L. Zhang, H.L. Chen, Pervaporation separation of xylene isomers by hybrid membranes of PAAS filled with silane-modified zeolite, Ind. Eng. Chem. Res. 49 (2010) 7504–7514.
[18] S.C. Kim, B.Y. Lim, Morphology and pervaporation characteristics of PAA/poly (BMA-co-MMA) IPN membranes, Front. Sep. Sci. Technol. 0 (2004) 12–15.
[19] S.C. Kim, B.Y. Lim, Preparation of composite membranes of dense PAA-poly (BMA-co-MMA) IPN supported on porous and crosslinked poly(BMA-co-MMA) sublayer and their pervaporation characteristics, Macromol. Res. 11 (2003) 163–171.
[20] P. Zhanga, J.W. Qian, Q.F. Ana, X.Q. Liua, Q. Zhao, H.T. Jina, Surface morphology and pervaporation performance of electric field enhanced multilayer membranes, J. Membr. Sci. 328 (2009) 141–147.
[21] S.Y. Nam, Y.M. Lee, Pervaporation and properties of chitosan-poly (acrylic acid) complex membranes, J. Membr. Sci. 135 (1997) 161–171.
[22] G. Dhanuja, B. Smitha, S. Sridhar, Pervaporation of isopropanol–water mixtures through polyion complex membranes, Sep. Purif. Technol. 44 (2005) 130–138.
[23] R.J. Samuels, Solid state characterization of the structure of chitosan films, J. Polym. Sci.: Polym. Phys. 19 (1981) 1081–1105.
[24] B. Focher, M. Tamagno Dave, E. Marsano, Hyaluronic acid-(hydroxypropyl)cellulose blends: A solution and solid state study, Macromolecules 28 (1995) 3531–3539.
[25] M.C. Burshe, S.B. Sawant, J.B. Joshi, V.G. Pangarkar, Sorption and permeation of binary water–alcohol systems through PVA membranes crosslinked with multifunctional crosslinking agents, Sep. Purif. Technol. 12 (1997) 145–156.
[26] C.J. Chen, Y. Deng, E.Y. Yan, Y. Hu, X.Q. Jiang, Preparation of porous chitosan-poly (acrylic acid)-calcium phosphate hybrid nanoparticles via mineralization, Chin. Sci. Bull. 54 (2009) 3127–3136.
[27] L.K. Pandey, C. Saxena, V. Dubey, Modification of poly(vinyl alcohol) membranes for pervaporative separation of benzene/cyclohexane mixtures, J. Membr. Sci. 227 (2003) 173–182.
[28] P. Kanti, K. Srigowri, J. Madhuri, B. Smitha, S. Sridhar, Dehydration of ethanol through blend membranes of chitosan and sodium alginate by pervaporation, Sep. Purif. Technol. 40 (2004) 259–266.
[29] H. Fujita, A. Kishimoto, K.M. Matsumoto, Concentration and temperature dependence of diffusion coefficients for systems poly(methyl acrylate) and n-alkyl acetates, Trans. Faraday Soc. 56 (1960) 424–432.
[30] S.S. Kulkarni, S.M. Tambe, A.A. Kittur, M.Y. Kariduraganavar, Modification of tetraethylorthosilicate crosslinked poly (vinyl alcohol) membrane using chitosan and its application to the pervaporation separation of water–isopropanol mixtures, J. Appl. Polym. Sci. 99 (2006) 1380–1389.
[31] H.M. Guan, T.S. Chung, Z. Huang, M.L. Chung, S. Kulprathipanja, Poly(vinyl alcohol) multilayer mixed matrix membranes for the dehydration of ethanol–water mixture, J. Membr. Sci. 268 (2006) 113–122.
[32] C.H. Lee, W.H. Hong, Influence of different degrees of hydrolysis of poly(vinyl alcohol) membrane on transport properties in pervaporation of IPA/water mixture, J. Membr. Sci. 135 (1997) 187–193.
[33] N.R. Singha, T.K. Parya, S.K. Ray, Dehydration of 1,4-dioxane by pervaporation using filled and cross-linked polyvinyl alcohol membrane, J. Membr. Sci. 340 (2009) 35–44.
[34] M.N. Hyder, R.Y.M. Huang, P. Chen, Composite poly (vinyl alcohol)–poly (sulfone) membranes cross-linked by trimesoyl chloride: Characterization and dehydration of ethylene glycol–water mixtures, J. Membr. Sci. 326 (2009) 363–371.